RESEARCH ARTICLE

Impact of pH on physicochemical properties of corn starch by dry heat treatment

Hwi Won Jung[1] · Hyun-Seok Kim[1,2]

Abstract

This study investigated the effects of temperature, pH, and starch genotype on starch characteristics after dry heat treatment (DHT). DHT starches were prepared according to 19 DHT conditions, constructed using a D-optimal design, and analyzed with respect to apparent amylose (AAM) content, X-ray diffraction (XRD) pattern, relative crystallinity (RC), solubility and swelling power (SP), thermal properties, and pasting viscosity. The DHT starches maintained their granular structures even after DHT at pH 3, although there was some damage to their granular surfaces. The DHT starches showed lower amylose content, RC, SP, gelatinization temperature and enthalpy, degree of retrogradation, and pasting viscosity, but higher solubility, compared to those of native starches. These DHT effects were more pronounced as pH decreased at each temperature, regardless of the starch genotype. Overall, DHT can be used to expand the physical functionality of high-amylose and highly crystallized starches with poor properties.

Keywords Physical starch modification · Dry heat treatment · Dry heat-treated starch · Physicochemical property · D-optimal design

Introduction

The chemical modifications (etherification, esterification, crosslinking, and oxidation) of starch are prevalent in the food and starch industries for improving and expanding their physical, thermal, and rheological properties (Choi and Kim, 2022). Recently, the food industry has attempted to avoid the use of chemically modified starches because of the strong opposition of consumers to chemically synthesized food additives (Kim and Kim, 2021). However, chemically modified starches cannot be completely excluded from processed foods because they significantly contribute to food processing, storage, and end-use quality (Obadi and Xu, 2021; Yousif et al., 2012). Thus, food manufacturers have

sought clean materials and technologies to replace chemically modified starches and their preparations.

Starches can be physically modified by heating, hydration, pressurization, shearing, or their combinations, without chemicals (e.g., catalysts and reacting agents) or chemical reactions (BeMiller and Huber, 2015; Fonseca et al., 2021). Thus, physical starch modification is of great interest as an alternative to chemical starch modification (BeMiller and Huber, 2015; Kim and Kim, 2021). For physically modified starches, native starches are subjected to heat-moisture treatment, dry heat treatment (DHT), annealing, heat- and pressure-induced pregelatization, extrusion, high-pressure homogenization, and ultra-fine pulverization (BeMiller and Huber, 2015; Ye et al., 2018). These commonly deform the inherent granular/crystalline structure and molecular arrangement of starches, ultimately altering their physical, thermal, and rheological properties (BeMiller and Huber, 2015; Ye et al., 2018). The commercial products of physically modified starches are currently known as clean-labeled starches and are frequently used as thickening and stabilizing agents for several food systems (e.g., sauce, yogurt, and instant soup premix) (Arocas et al., 2009; Park and Kim, 2021). This is because the functions of physically modified starches do not correspond to or exceed those of chemically

✉ Hyun-Seok Kim
khstone@kyonggi.ac.kr

Hwi Won Jung
gnldnjs0210@naver.com

[1] Department of Food Science and Biotechnology, Graduate School, Kyonggi University, Suwon 16227, Korea

[2] Major of Food Science and Biotechnology, Division of Bio-Convergence, Kyonggi University, Suwon 16227, Korea

modified starches (Kim and Kim, 2021). Therefore, many studies have been conducted on physical modification methods to improve the physicochemical properties of physically modified starches.

DHT is mainly involved in the semi-dry heat reaction (SDHR) for the preparation of phosphorylated (Sitohy et al., 2000), carboxylated (Hong et al., 2020), and pyroconverted (Weil et al., 2020) starches and starch-anionic hydrocolloid composites (Lim et al., 2002; 2003). However, the modification efficacy of modified starches subjected to SDHR based on DHT is either underestimated or overestimated because of the lack of information on the effects of DHT on starch characteristics. Therefore, it is difficult to develop a modification method that is acceptable in the food industry. DHT, as a physical modification method for starch, is simple, safe, and inexpensive and does not require any specific reactors or equipment (Gou et al., 2019; Liu et al., 2019; Qiu et al., 2015; Qin et al., 2016; Sun et al., 2014; Zhou et al., 2021). Several studies have investigated the effects of DHT on the physicochemical properties of quinoa (Zhou et al., 2021), proso millet (Sun et al., 2014), sweet potato (Gou et al., 2019), waxy potato (Liu et al., 2019), and waxy rice (Qiu et al., 2015; Qin et al., 2016) starches. They reported that DHT significantly affected the relative crystallinity, solubility, swelling power, gelatinization temperature and enthalpy, and pasting viscosity of starch. However, the effects of temperature and time on these characteristics differed between the starch sources. These inconsistent results may be because starch pH is not considered a factor in DHT. pH directly affects the pasting viscosities of native starches (Shi and BeMiller, 2002) and the formation and characteristics of starch-anionic hydrocolloid composites (Lim et al., 2003).

Therefore, the objective of this study was to investigate the effects of pH on the physicochemical properties of DHT starches. To achieve this objective, this study examined the effect of interactions between pH and temperature and between pH and starch genotype on the characteristics of DHT starches using a D-optimal design and response surface methodology (RSM). Normal and waxy corn starches were used as starch sources in this study because they are widely used in the food and starch industries worldwide.

Materials and methods

Materials

Normal and waxy corn starches, designated as NST and WST, respectively, were purchased from Daesang Co. (Seoul, Korea) and used without further purification. All chemicals and reagents used in this study were of ACS grade.

Experimental design

Nineteen experimental conditions were generated according to a D-optimal design using Design Expert (version 8.0.6, State-Ease, Inc., Minneapolis, MN, USA) to prepare the DHT starches (Alimi et al., 2013). The design consisted of two numerical factors (temperature and pH) and one categorical factor (starch genotype) as independent variables to investigate the effect of pH and interactions between pH and temperature and between pH and starch genotype on the characteristics of DHT starches. The levels (determined from the preliminary study) of the factors were 130–170 °C for temperature, 3–7 for pH, and normal and waxy for starch genotypes. The D-optimal design matrix with the factors and their actual levels is listed in Table 1. The dependent variables (response) were apparent amylose content, relative crystallinity, solubility, swelling power, gelatinization temperature and enthalpy, degree of retrogradation, and pasting viscosity parameters. The measured responses are listed in Table 1.

Dry heat treatment of starch

Starch (50 g, d.b or dry weight basis) was dispersed in deionized water (DIW, 1000 mL) and adjusted to the predetermined pH using 0.1 N HCl or 0.1 N NaOH. The starch was recovered using a Büchnel funnel and dried at 45 °C until its moisture content was below 7.5% (approximately 48 h). The dried starch cake was blended, passed through a 60-mesh standard sieve (No. 60; Chunggye Co., Seoul, Korea), and heated for 4 h in a convection oven (OF-22; JeioTech, Daejeon, Korea) at a predetermined temperature. To establish a control for the DHT starch, starch was adjusted to pH 7 using 0.1 N NaOH and subjected to the same procedure, except for the dry heat treatment.

Characteristics of DHT starch

The morphological characteristics of the starch were observed using a scanning electron microscope (SNE-3000 MB; SEC Co., Ltd., Suwon, Korea) at an accelerating voltage of 30 kV and 600 × magnification (Kim and Kim, 2021). The apparent amylose content was measured using a colorimetric method (Chrastil, 1987). X-ray diffraction pattern and relative crystallinity were investigated using an X-ray diffractometer (D8 Advance; Bruker, Billerica, MA, USA) according to the method outlined by Bae et al. (2020). The swelling power and solubility were measured at 85 °C according to the method outlined by Hong et al. (2020). Gelatinization and melting properties were investigated using a differential scanning calorimeter (DSC4000;

Table 1 D-optimal design matrix for preparation of the dry heat-treated starches and their characteristics

Run	Temperature (°C)	pH	Genotype	AAM (%, d.b)	RC (%)	Sol (%, d.b)	SP (g/g)	T_o (°C)	T_p (°C)	T_e (°C)	ΔH (J/g)	DR (%)	PV (mPa·s)	TV (mPa·s)	BD (mPa·s)	FV (mPa·s)	SB (mPa·s)
R01	130	7	NST	29.4±0.2	20.3±0.1	4.4±0.3	10.5±0.0	64.4±0.2	68.7±0.2	75.0±0.5	14.0±0.2	49.1±3.7	1424.0±15.6	869.0±5.7	555.0±21.2	1235.5±24.7	366.5±30.4
R02	150	7	WST	2.2±0.2	19.8±0.0	45.2±0.4	1.5±0.1	63.9±0.0	70.0±0.0	77.4±0.0	12.3±0.0	50.4±2.9	1617.0±7.1	851.0±1.4	766.0±8.5	1054.5±7.8	203.5±9.2
R03	150	7	NST	28.0±0.8	19.0±0.1	6.0±0.1	5.9±0.3	63.6±0.3	67.9±0.4	74.1±0.4	14.0±0.1	40.6±1.3	1288.5±17.7	793.0±22.6	495.5±5.0	1026.0±21.2	233.0±1.4
R04	170	5	WST	2.0±0.3	19.9±0.0	45.2±0.4	0.9±0.0	62.0±0.2	67.8±0.1	74.3±0.3	8.7±0.3	36.3±2.8	103.5±2.1	40.0±1.4	63.5±0.7	58.5±0.7	18.5±0.7
R05	170	3	WST	0.7±0.0	18.6±0.1	55.2±0.5	0.3±0.1	45.3±0.0	51.2±0.1	57.7±0.4	2.3±0.1	7.0±1.1	0.0±0.0	0.0±0.0	0.0±0.0	0.0±0.0	0.0±0.0
R06	150	7	WST	2.2±0.1	19.7±0.1	45.8±0.4	1.6±0.1	63.8±0.0	70.0±0.0	77.4±0.0	12.3±0.0	51.4±1.4	1614.5±3.5	851.5±0.7	763.0±4.2	1051.8±3.9	200.3±4.6
R07	150	5	NST	27.7±0.1	19.4±0.2	11.2±0.6	7.6±0.1	62.8±0.1	67.2±0.1	73.1±1.2	12.9±0.5	36.6±0.4	817.0±18.4	373.0±4.2	444.0±14.1	537.0±8.5	164.0±4.2
R08	130	3	NST	26.9±0.0	21.6±0.4	10.1±0.2	9.3±0.2	64.4±0.2	68.8±0.1	75.1±0.0	13.3±0.2	32.2±0.8	641.0±24.0	237.0±5.7	404.0±18.4	375.0±11.3	138.0±5.7
R09	150	3	WST	1.2±0.3	19.1±0.1	51.6±0.2	0.4±0.1	55.3±0.0	62.4±0.1	77.4±0.1	11.4±0.4	12.1±1.1	4.5±0.7	0.0±0.0	4.5±0.7	4.0±4.2	4.0±4.2
R10	170	5	WST	1.9±0.2	19.9±0.0	45.8±0.4	0.8±0.0	61.7±0.2	68.0±0.1	74.8±0.3	9.1±0.3	40.2±2.8	103.5±2.1	40.0±1.4	63.5±0.7	58.5±0.7	18.5±0.7
R11	170	3	NST	6.9±0.1	18.0±0.2	52.0±0.9	0.2±0.0	50.1±0.1	61.5±0.3	72.3±0.1	0.9±0.0	25.9±3.4	0.0±0.0	0.0±0.0	0.0±0.0	0.0±0.0	0.0±0.0
R12	130	5	WST	2.6±0.1	23.3±0.1	48.7±0.1	1.9±0.0	66.2±0.1	72.1±0.0	78.2±0.1	15.1±0.4	45.8±1.1	1704.0±5.7	812.0±11.3	892.0±5.7	1015.5±7.8	203.5±3.5
R13	130	5	WST	2.7±0.0	23.4±0.1	48.8±0.0	1.9±0.0	66.1±0.1	72.1±0.0	78.4±0.1	15.7±0.4	44.3±1.1	1702.0±2.8	808.0±5.7	894.0±2.8	1012.8±3.9	204.8±1.8
R14	130	3	WST	1.8±0.2	19.7±0.1	50.5±0.6	0.6±0.1	64.8±0.2	70.9±0.0	79.8±4.1	13.0±0.7	39.8±4.1	191.5±5.0	31.5±9.2	160.0±4.2	48.0±4.2	16.5±5.0
R15	150	5	NST	27.7±0.0	19.4±0.0	11.0±0.3	7.6±0.0	63.0±0.2	66.9±0.3	70.6±2.3	11.9±0.9	36.4±0.2	823.5±9.2	374.5±2.1	449.0±7.1	540.0±4.2	165.5±2.1
R16	150	5	NST	27.6±0.0	19.4±0.1	11.4±0.3	7.6±0.0	62.9±0.1	67.2±0.1	73.0±1.1	12.9±0.5	36.7±0.2	810.5±9.2	371.5±2.1	439.0±7.1	534.0±4.2	162.5±2.1
R17	170	5	NST	25.2±0.6	19.4±0.1	24.9±0.7	5.9±0.3	58.3±0.1	63.2±0.1	70.5±0.5	11.6±0.1	34.6±1.0	141.0±38.2	58.0±9.9	83.0±28.3	91.0±14.1	33.0±4.2
R18	150	5	WST	2.5±0.0	19.3±0.1	55.7±0.7	1.3±0.0	64.8±0.3	70.8±0.0	77.3±0.2	12.7±0.6	45.0±0.0	870.0±1.4	368.5±0.7	501.5±2.1	449.0±2.8	80.5±2.1
R19	170	7	NST	27.1±0.1	17.2±0.1	11.3±0.2	7.1±0.1	61.0±0.1	65.0±0.1	71.0±0.1	11.7±0.3	37.0±2.6	410.0±22.6	286.0±19.8	124.0±2.8	392.0±15.6	106.0±4.2
Native NST				36.4±1.3	21.7±0.5	3.3±0.0	11.8±0.3	66.4±0.2	70.6±0.1	76.3±0.3	15.7±1.0	53.0±1.0	1407.5±41.7	1015.0±29.7	392.5±12.0	1486.5±67.2	471.5±37.5
Native WST				3.0±0.2	24.7±0.1	28.6±0.9	9.8±0.7	67.6±0.4	73.2±0.2	79.7±0.4	18.3±0.2	55.2±0.5	2323.0±9.9	1161.0±7.1	1162.0±17.0	1345.5±13.4	184.5±20.5

Mean value of three replicate measurements

AAM apparent amylose; *RC* relative crystallinity, *WHC* water holding capacity, *Sol* solubility, *SP* swelling power, T_o gelatinization onset temperature, T_c gelatinization completion temperature, T_p gelatinization peak temperature, T_e gelatinization completion temperature, *ΔH* gelatinization enthalpy, *DR* degree of retrogradation, *PV* peak viscosity, *BD* breakdown viscosity, *TV* trough viscosity, *FV* final viscosity, *SB* setback viscosity, *NST* normal corn starch, *WST* waxy corn starch

PerkinElmer, Waltham, MA, USA) according to the method outlined by Choi and Kim (2022). The degree of retrogradation was calculated as the percentage ratio of melting to gelatinization enthalpy (Bae et al., 2020). Pasting viscosity profiles and characteristics were examined using Rapid Visco Analyzer (RVA-3D; Newport Scientific, NSW, Australia) according to the operating conditions and programmed temperature profiles described by Hong et al. (2020).

Statistical analysis

The DHT starch was prepared three times in every experimental condition, and its physicochemical properties were analyzed twice for each DHT starch. One-way analysis of variance was performed using the measured data, and the significance of the physicochemical properties between the DHT starches was investigated using Tukey's HSD multiple range test at $p < 0.05$. Statistical computations and analyses were performed using Minitab 18 (Minitab Inc., State College, PA, USA). In addition, RSM was conducted with the mean values of each physicochemical property of the DHT starch using Design Expert (version 8.0.6, State-Ease, Inc., Minneapolis, MN, USA).

Results and discussion

Morphological characteristic

The scanning electron microscope (SEM) images of the native and DHT starches are shown in Fig. S1 (in the Supplementary Data). The native NST and WST showed polygonal and round granules with smooth surfaces, consistent with the literature (Choi and Kim, 2022). Uneven erosion, bumps, dents, and cracks were observed on the surfaces of the DHT starch granules. These changes were more pronounced as the temperature increased at each pH and the pH

decreased at each temperature (Fig. S1). These results were consistent with those reported by Gou et al. (2019), Liu et al. (2019), Mao et al. (2021a; 2021b), Qiu et al. (2015), Sun et al. (2014), and Zhou et al. (2021). Liu et al. (2019) suggested that the distinct surface structures could be attributed to the discharge of hot vapor from the relatively moisture-rich region of the granules during DHT, leading to partial swelling and gelatinization in those regions. Distorted surface structures were more frequently observed in DHT-WST than in DHT-NST (Fig. S1). This may be because WST has no or very low amylose that enhances granule rigidity (Kim et al., 2012), being easily damaged by DHT. Overall, damage to the granular structure of the starch by DHT was evident, which might weaken the stability and integrity of the starch granules.

Apparent amylose (AAM) content

The AAM contents of the DHT starches are listed in Table 1, and the interaction plots from the RSM analysis are shown in Fig. 1. The AAM contents were in the ranges of 6.9–29.4% and 0.7–2.7% for the DHT-NST and DHT-WST, respectively, and were significantly lower than those of their native counterparts (36.4% for NST and 3.0% for WST) (Table 1). This result indicates that DHT degrades amylose molecules (Mao et al., 2021a; 2021b). A quadratic regression model was fitted to explain the effects of the DHT parameters (temperature, pH, and genotype) on the AAM content of the DHT starches (Table 2). The AAM content was significantly affected by the main factors (temperature, $p < 0.05$; pH, $p < 0.01$; genotype, $p < 0.01$) and the interactions ($p < 0.01$) between temperature and pH, temperature and genotype, and pH and genotype (Table 2). The AAM content of the DHT-NST decreased with decreasing pH at each temperature, and this trend became more pronounced as the temperature increased (Fig. 1). This suggests that starch pH affects the dextrinization of amylose molecules by DHT (Mao et al., 2021a; 2021b). A similar trend was observed in
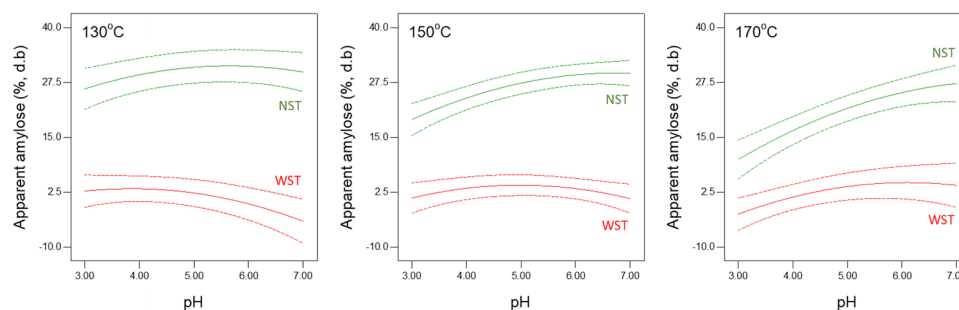

Fig. 1 Interaction plots describing the effects of dry heat treatment on the apparent amylose content of starch (NST, normal corn starch; WST, waxy corn starch). Solid lines indicate the predicted apparent amylose contents from the RSM analysis and the dashed lines around the solid line represents the confidence interval of the predicted regression plot

Table 2 Significance of the regression models (F-value) and the effects of variables on characteristics of the dry heat-treated starches

Source Model	AAM Quadratic	RC Quadratic	Sol 2FI	SP 2FI	T_o Quadratic	T_p Linear	T_c Linear	ΔH Quadratic	DR 2FI	PV 2FI	TV 2FI	BD 2FI	FV 2FI	SB 2FI
Regression	73.3**	9.2**	66.6**	26.4**	21.8**	7.0**	4.1*	20.2**	8.9**	25.6**	32.3**	16.8**	40.4**	84.1**
A	8.0*	44.5**	11.2**	15.2**	54.3**	13.5**	8.8**	62.9**	8.4**	68.1**	71.6**	50.9**	97.0**	231.9**
B	12.4**	0.6	30.5**	7.3*	42.4**	6.6*	1.4	26.3**	34.3**	70.3**	110.7**	32.1**	133.6**	217.3**
C	500.4**	4.7	288.4**	117.2**	0.1	0.8	1.8	0.1	0.8	2.4	1.3	3.0	0.0	30.3**
AB	12.3**	0.5	17.5**	3.7	28.2**	–	–	20.3**	0.7	7.2*	12.7**	2.7	15.7**	28.1**
AC	15.0**	0.2	30.3**	13.8**	1.3	–	–	0.0	0.6	2.3	1.9	2.1	0.8	4.3
BC	13.8**	4.2	8.5*	1.1	1.9	–	–	3.5	6.4*	10.0**	5.3*	12.4**	4.9*	1.6
A²	0.9	9.4*	–	–	0.1	–	–	2.1	–	–	–	–	–	–
B²	8.4*	12.0**	–	–	22.2**	–	–	14.7**	–	–	–	–	–	–
Lack of fit	300.4**	294.0**	368.5**	1205.8**	304.3**	1399.4**	27.6**	15.9**	33.5**	2243.6**	654.3**	847.2**	846.7**	30.3**
r²	0.983	0.880	0.971	0.930	0.946	0.583	0.451	0.942	0.817	0.928	0.942	0.894	0.953	0.977
Adjusted r²	0.970	0.784	0.956	0.895	0.903	0.499	0.341	0.895	0.725	0.891	0.912	0.841	0.929	0.965

AAM apparent amylose, *RC* relative crystallinity, *WHC* water holding capacity, *Sol* solubility, *SP* swelling power, T_o gelatinization onset temperature, T_p gelatinization peak temperature, T_c gelatinization completion temperature, *ΔH* gelatinization enthalpy, *DR* degree of retrogradation, *PV* peak viscosity, *TV* trough viscosity, *BD* breakdown viscosity, *FV* final viscosity, *SB* setback viscosity

A temperature, B pH, C genotype

$*p < 0.05$, $**p < 0.01$

the DHT-WST depending on the combination of temperature and pH; however, the variation was much less pronounced than that observed in DHT-NST, owing to the lower AAM content of WST (Fig. 1). This implies that the degradation of starch molecules by DHT dominates that of amylose rather than amylopectin (Mao et al., 2021a; 2021b).

X-ray diffraction (XRD)

The XRD patterns of the DHT starches are shown in Fig. S2 (in the Supplementary Data). The relative crystallinity (RC) of the DHT starches is listed in Table 1, and a one factor plot from the RSM analysis is shown in Fig. S3 (in the Supplementary Data). The native NST and WST exhibited typical A-type crystal packing arrangements with strong peak intensities at 15°, 17°, 18°, and 23° 2θ (Hong et al., 2020). However, in the DHT starches, the split peaks observed in the native NST and WST at 17–18° 2θ became blunt and finally combined to form one peak as the temperature increased at each pH condition. In addition, the intensities of all crystal peaks were significantly reduced. The observed patterns were more pronounced as the pH decreased (Fig. S2 in the Supplementary Data). This result is similar to that of the DHT starches reported by Liu et al. (2019) and Mao et al. (2021a; 2021b) but differs from that of the crystalline structures of rice (Qiu et al., 2015; Qin et al., 2016), quinoa (Zhou et al., 2021), and proso millet (Sun et al., 2014) starches, which remained unchanged after DHT. This inconsistency may be because of the differences in the number of crystals within the starch before and after DHT. For example, the RC of the proso millet starch decreased to 36.3–37.9% after DHT compared with that (41.2%) of the untreated starch, indicating some alterations in the crystalline structure after DHT (Sun et al., 2014). However, the A-type XRD pattern was still observed in the DHT starches (Sun et al., 2014). This implies that there were sufficient intact crystals to represent the A-type crystalline pattern by XRD. Accordingly, the distorted XRD patterns observed in this study might be attributed to the lack of intact crystals in the DHT-NST and DHT-WST, with an RC of 17.2–21.6% and 18.6–23.4%, respectively (Table 1).

As previously described, the RCs of the DHT-NST and DHT-WST were lower than those of the native NST (21.7%) and WST (24.7%) (Table 1). A quadratic regression model was used to describe the effects of DHT on the RCs of the DHT starches (Table 2). RC was significant in the linear ($p < 0.01$) and quadratic ($p < 0.05$) terms of temperature and the quadratic term of pH ($p < 0.01$); however, no interaction was observed between the main factors (Table 2). The RC of the DHT starches decreased with increasing temperature, regardless of the starch genotype (Fig. S3 in the Supplementary Data). This result is consistent with those reported by

Liu et al. (2019), Mao et al. (2021a; 2021b), and Sun et al. (2014). They attributed the RC reduction of DHT starches to the disintegration and movement of amylopectin double helices, along with the evaporation of water molecules deposited within amylopectin clusters by DHT. In contrast, Qiu et al. (2015), Qin et al. (2016), and Zhou et al. (2021) reported a significant increase in the RC of DHT starches resulting from the rearrangement and recrystallization of disrupted amylopectin double helices during and after DHT. Previous studies indicated an early event in which DHT damaged the crystalline structure of starch. Moreover, DHT, in the presence of an acid or under acidic pH conditions, invariably reduces the RC of starch (Mao et al., 2021a; 2021b; Weil et al., 2020). Accordingly, it is clear that pH contributes to the reduction of starch RC by DHT, although the effect of pH on RC was not significant in this study.

Solubility and swelling power (SP)

The solubility and SP of the DHT starches are presented in Table 1, and their interaction plots obtained from the RSM analysis are shown in Fig. 2. The solubilities of the DHT-NST and DHT-WST were in the ranges of 4.4–52.0% and 45.2–55.7%, respectively, and were significantly higher than those of the native NST (3.3%) and WST (28.6%) (Table 1). A two factor interaction (2FI) model well explained the effects of the DHT parameters on the solubility of the DHT starches (Table 2). Solubility was significantly affected by the main factors (temperature, $p < 0.01$; pH, $p < 0.01$; genotype, $p < 0.01$) and the interactions between temperature and pH ($p < 0.01$), temperature and genotype ($p < 0.01$), and pH and genotype ($p < 0.05$) (Table 2). At each temperature, the solubility of the DHT-NST increased as pH decreased, and this pattern became more pronounced with increasing temperature (Fig. 2). In the DHT-WST, solubility exhibited only minute changes depending on the pH at 130 °C and 150 °C, whereas solubility noticeably decreased with pH at 170 °C (Fig. 2). This may be because of the narrower range of the solubility of the DHT-WST (45.2–55.7%) than that of the DHT-NST (4.4–52.0%). Overall, these results are in good agreement with those reported by Gou et al. (2019), Liu et al. (2019), Mao et al. (2021a; 2021b), and Zhou et al. (2021). The higher solubility of the DHT starches in this study may be ascribed to the dextrinization of starch molecules (predominantly amylose) and destruction of starch crystallites by DHT, facilitating the leaching of starch molecules and their hydrolysates from the swollen granules (Gou et al., 2019; Liu et al., 2019; Mao et al., 2021a; 2021b; Zhou et al., 2021).

The SPs of the DHT-NST and DHT-WST were in the ranges of 0.2–10.5 g/g and 0.3–1.9 g/g, respectively, and were significantly lower than those of the native NST (11.8 g/g) and WST (9.8 g/g) (Table 1). Similar to their

Fig. 2 Interaction plots describing the effects of dry heat treatment on the solubility and swelling power of starch (NST, normal corn starch; WST, waxy corn starch). Solid lines indicate the predicted solubility and swelling power from the RSM analysis and the dashed lines around the solid line represents the confidence interval of the predicted regression plot
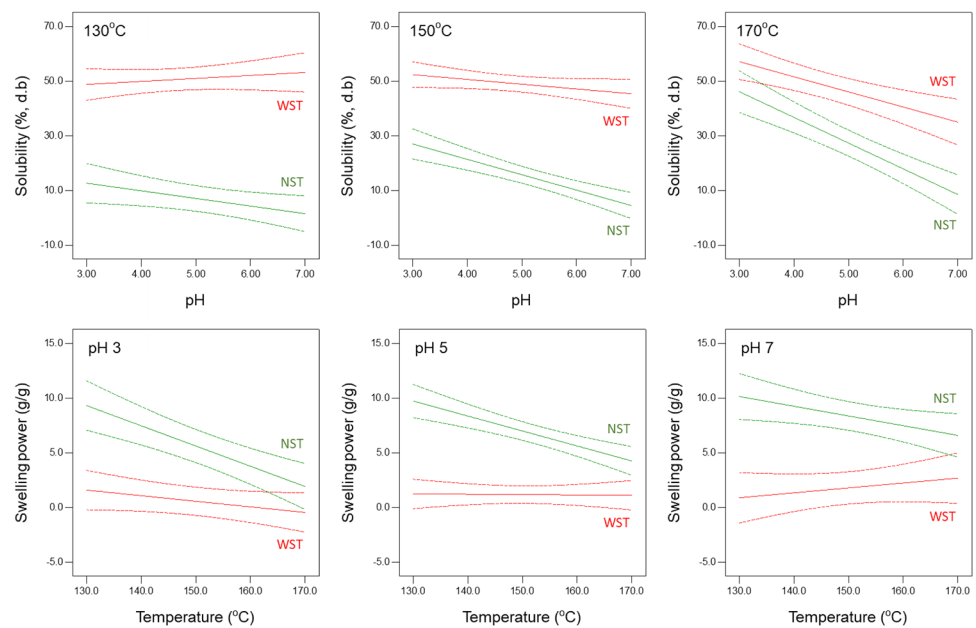

solubilities, the 2FI model well described the effects of the DHT parameters on the SP of DHT starches (Table 2). SP was significantly affected by the main factors (temperature, $p < 0.01$; pH, $p < 0.05$; genotype, $p < 0.01$) and the interaction between temperature and genotype ($p < 0.01$) (Table 2). A dramatic change in SP was observed only in the DHT-NST; its SP decreased with the temperature at each pH and increased with pH at each temperature (Fig. 2). However, the DHT-WST exhibited no pronounced changes in SP with changing temperature or pH (Fig. 2). This may be because of the lower SP and narrower SP range of the DHT-WST compared with those of the DHT-NST. The lower SP values of the DHT starches in this study are consistent with those reported by Gou et al. (2019), Liu et al. (2019), Mao et al. (2021a; 2021b), and Zhou et al. (2021). The DHT starches retained their granular structures, but the granules showed surface erosion, partial swelling in certain areas, and irregular cracks, indicating damage to the granular structures by DHT (Fig. S1 in the Supplementary Data). DHT dextrinizes amylose molecules that restrict starch swelling and ensure the integrity of swollen starch granules (Choi and Kim, 2022; Kim and Huber, 2010) and partially destructs starch crystallites that also inhibit starch swelling (Liu et al., 2019; Mao et al. 2021a; 2021b), destabilizing the granular structure of DHT starches. Consequently, the weakened granular structure of DHT starches facilitates the rupture of their granules during heating in water, resulting in lower SP and higher solubility (Liu et al., 2019; Mao et al., 2021a; 2021b). This was noticeable

when the starch was subjected to DHT at a high temperature and low pH.

Thermal property

The gelatinization temperatures and enthalpies of the DHT starches are listed in Table 1. The gelatinization onset, peak, and completion temperatures of the DHT-NST and DHT-WST were significantly lower than those of their native NST and WST, respectively (Table 1). This result is consistent with those reported by Gou et al. (2019), Liu et al. (2019), and Zhou et al. (2021). The downward shift in the gelatinization temperature was attributed to the weakened granular structure of the DHT starches and damage to starch crystallites by DHT, as previously explained (Gou et al., 2019; Liu et al., 2019; Zhou et al., 2021). The gelatinization onset temperature was well explained by the quadratic regression model ($p < 0.01$), whereas the gelatinization peak ($p < 0.01$) and completion ($p < 0.05$) temperatures were fitted to the linear regression model (Table 2). The gelatinization onset temperature was significantly affected by temperature ($p < 0.01$), pH ($p < 0.01$), the interaction between temperature and pH ($p < 0.01$), and the quadratic term of pH ($p < 0.01$) (Table 2). Regardless of the starch genotype, there was no significant change in the gelatinization onset temperature at pH 7, whereas a dramatic reduction was found at pH 3 (Fig. 3). The gelatinization peak temperature was significantly affected by temperature ($p < 0.01$) and pH ($p < 0.01$) (Table 2). It decreases with increasing temperature and increases with increasing pH (Fig. 3).

Fig. 3 Interaction (gelatinization onset temperature, gelatinization enthalpy, and degree of retrogradation) and one factor (gelatinization peak and completion temperatures) plots describing the effects of dry heat treatment on the thermal property of starch (NST, normal corn starch; WST, waxy corn starch). Solid lines indicate the predicted thermal properties from the RSM analysis and the dashed lines around the solid line represents the confidence interval of the predicted regression plot
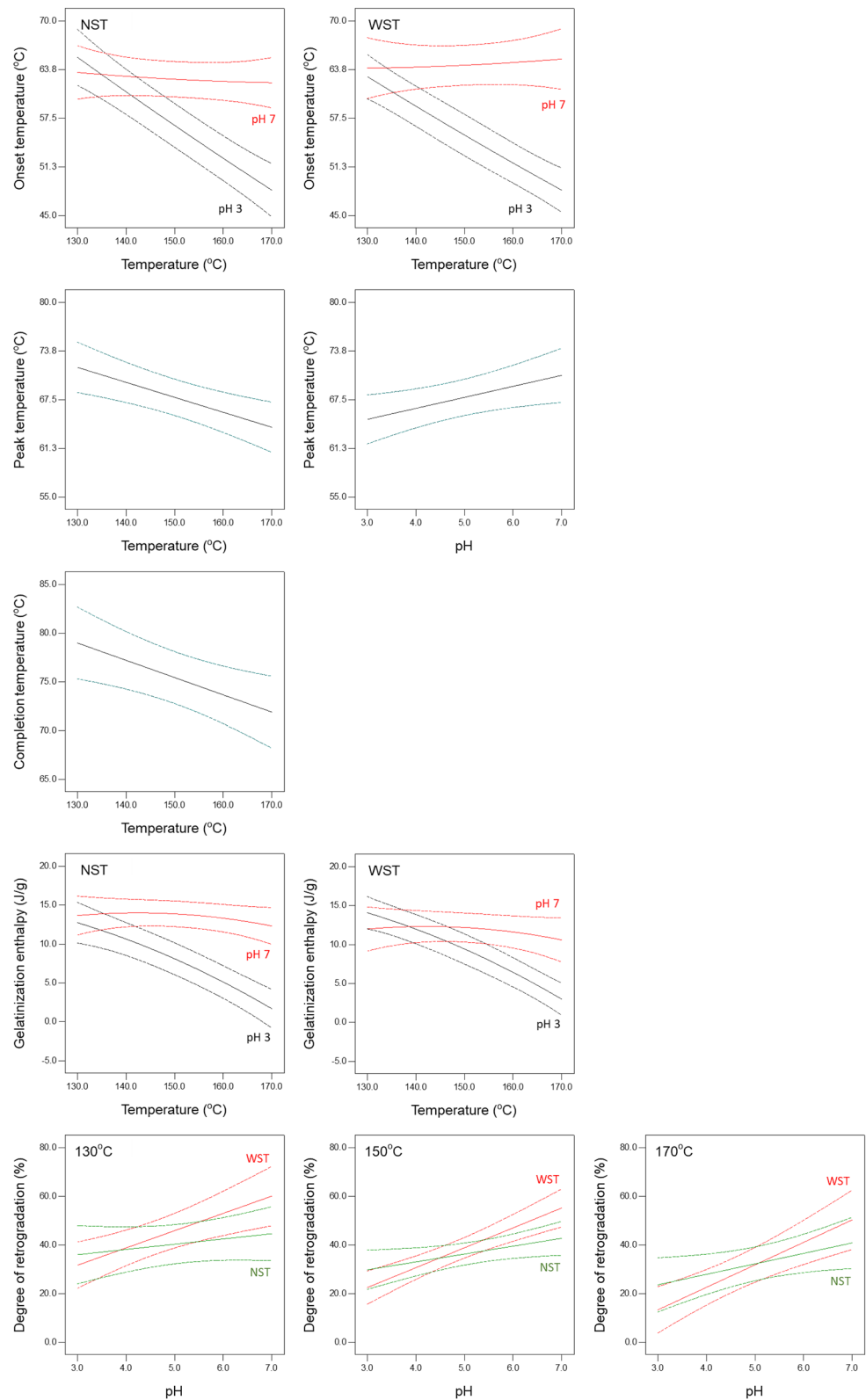
The gelatinization completion temperature was significantly affected only by temperature ($p < 0.01$) (Table 2), and it decreased with increasing temperature (Fig. 3).

The gelatinization enthalpies of the DHT-NST and DHT-WST were in the ranges of 0.9–14.0 J/g and 2.3–15.7 J/g, respectively, and were significantly lower than those of the

native NST (15.7 J/g) and WST (18.3 J/g) (Table 1). This is attributed to the lower RC of the DHT starches (Gou et al., 2019; Liu et al., 2019; Mao et al., 2021a; 2021b; Zhou et al., 2021). The gelatinization enthalpy was well explained by the quadratic regression model ($p < 0.01$) and was significantly affected by the linear term of temperature ($p < 0.01$), linear and quadratic terms of pH ($p < 0.01$), and interaction between temperature and pH ($p < 0.01$) (Fig. 2). There was no significant change in the gelatinization enthalpy with changing temperature at pH 7, regardless of the starch genotype. However, the gelatinization enthalpy dramatically decreased with increasing temperature at pH 3, and its altitude was higher for the DHT-WST than for the DHT-NST (Fig. 3). Considering that the gelatinization enthalpy is directly associated with starch RC (Choi and Kim, 2022; Kim and Huber, 2010), it is evident that fatal damage to the crystalline structure of starch is caused by DHT at acidic pH, although no direct relationship was found between pH and RC in this study (Table 2).

The DRs of the DHT-NST and DHT-WST were in the ranges of 25.9–49.1% and 7.0–51.4%, respectively, and were significantly lower than those of the native NST (53.0%) and WST (55.2 J/g) (Table 1). The DR was well fitted to the 2FI regression model ($p < 0.01$) and was significantly affected by the linear terms of temperature ($p < 0.05$) and pH ($p < 0.01$) and the interaction between pH and starch genotype ($p < 0.05$) (Fig. 2). The DR of the DHT-NST gradually increased with increasing pH at each temperature, whereas a dramatic increase in DR was observed in the DHT-WST (Fig. 3). Regardless of the starch genotype, the DR decreased with the temperature at each pH (Fig. 3). The DR measured in this study can indirectly explain the effect of DHT on the rearrangement and recrystallization of amylopectin rather than the reassociation of amylose, owing to the long-term retrogradation of the native and DHT starch pastes subjected to storage for 4 weeks at 4 °C. As mentioned previously, DHT hydrolyzes amylose and amylopectin molecules via pyroconversion and destroys the crystal packing arrangement and starch crystallites. These phenomena became more pronounced as the pH of the starch decreased. Thus, the lower DR of the DHT starches may be attributed to the significant damage to starch molecules and crystallites, resulting in the retardation or restriction of the rearrangement and recrystallization of amylopectin molecules and crystal remnants (Han et al., 2018; Mao et al., 2021a; 2021b; Weil et al., 2020).

Pasting viscosity property

The pasting viscosity profiles and characteristics of the DHT starches are shown in Fig. S4 (in the Supplementary Data) and Table 1, respectively. The pasting viscosity profiles of the DHT starches were successfully obtained at the tested temperatures at pH 5 and 7, but not at pH 3, except for the DHT-NST, which was tested at 130 °C and pH 3 (Fig. S4 in the Supplementary Data). The altitude of the pasting viscosity profile decreased as the temperature increased and the pH decreased (Fig. S4 in the Supplementary Data). This result was consistent with those reported by Gou et al. (2019), Lim et al. (2002), Sun et al. (2014), and Qiu et al. (2015). The DHT-NST and DHT-WST exhibited lower peak, trough, breakdown, final, and setback viscosities than did their native NST and WST (Table 1), except for the setback viscosity of DHT-WST prepared at 130 °C and pH 5 (R12 and R13 in Table 1) and at 150 °C and pH 7 (R02 and R06 in Table 1). The 2FI regression model well explained the effects of DHT on the peak, trough, breakdown, final, and setback viscosities of starch ($p < 0.01$) (Table 2). The peak, trough, and final viscosities were significantly affected by the linear terms of temperature ($p < 0.01$) and pH ($p < 0.01$) and the interactions between temperature and pH ($p < 0.05$ for peak viscosity and $p < 0.01$ for trough and final viscosities) and between pH and starch genotype ($p < 0.01$ for peak viscosity and $p < 0.05$ for trough and final viscosities) (Table 2). The breakdown viscosity was significant in the linear terms ($p < 0.01$) of temperature and pH and the interaction between pH and starch genotype ($p < 0.01$) (Table 2). The setback viscosity was significant in the linear terms ($p < 0.01$) of temperature, pH, and starch genotype and the interaction between temperature and pH ($p < 0.01$) (Table 2). The interaction plots of the peak, trough, breakdown, final, and setback viscosities obtained from the RSM analysis showed that the viscosities decreased as temperature increased and pH decreased (Fig. 4). This is because the dextrinization of starch molecules, partial destruction of starch crystallites, and weakening of starch granules by DHT result in the rapid and easy rupture of swollen granules by continued shear during RVA testing, finally reducing the pasting viscosities (Gou et al., 2019; Lim et al., 2002; Sun et al., 2014; Qiu et al., 2015).

In conclusion, this study investigated the effects of DHT parameters (temperature, pH, and starch genotype) on starch characteristics. DHT reduced the AAM content, XRD pattern, RC, SP, gelatinization temperature and enthalpy, DR, and pasting viscosity of the starch, whereas it enhanced starch solubility. This was much more pronounced as the starch pH decreased. Therefore, pH should be considered the most important factor when using starch materials as thickeners in food preparation. DHT is a modification method used to improve the characteristics of high-amylose and highly crystalline starches, which commonly exhibit poor properties. In addition, DHT starch prepared under acidic conditions has high solubility and low viscosity, similar to those of oxidized starch. In the noodle industry, oxidized starch is commonly dusted on fresh noodles to prevent their adhesion and is completely removed during the washing of

Fig. 4 Interaction plots describing the effects of dry heat treatment on the pasting viscosity property of starch (NST, normal corn starch; WST, waxy corn starch). Solid lines indicate the predicted pasting viscosity properties from the RSM analysis and the dashed lines around the solid line represents the confidence interval of the predicted regression plot
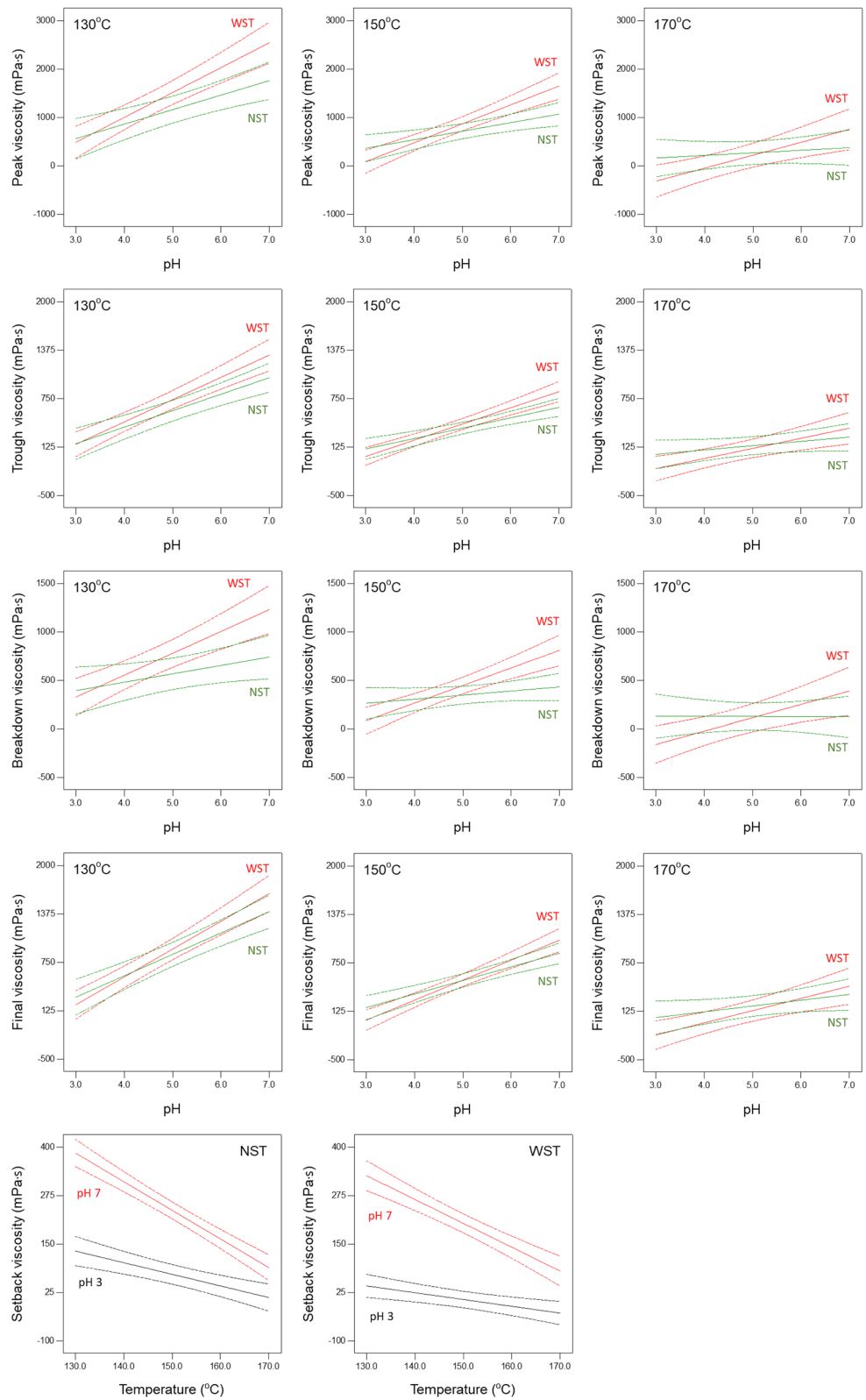
cooked noodles. Accordingly, the DHT starch can be used as an alternative to oxidized starch as a dusting agent in noodle making.

Declarations

Conflict of interest The authors declare no conflict of interest.

References

Alimi M, Mizani M, Naderi G, Shokoohi S. Effect of inulin formulation on the microstructure and viscoelastic properties of low-fat mayonnaise containing modified starch. Journal of Applied Polymer Science. 130: 801-809 (2013)

Arocas A, Sanz T, Fiszman SM. Clean label starches as thickeners in white sauce. Shearing, heating and freeze/thaw stability. Food Hydrocolloids. 23: 2031-2037 (2009)

Bae JE, Hong JS, Baik MY, Choi HD, Choi HW, Kim HS. Impact of starch granule-associated surface and channel proteins on physicochemical properties of corn and rice starches. Carbohydrate Polymers. 250: 116908 (2020)

BeMiller JN, Huber KC. Physical modification of food starch functionalities. Annual Review of Food Science and Technology. 6: 19-69 (2015)

Choi HW, Kim HS. Hydroxypropylation and acetylation of rice starch: effects of starch protein content. Food Science and Biotechnology. 31: 1169-1177 (2022)

Chrastil J. Improved colorimetric determination of amylose in starches or flours. Carbohydrate Research. 159: 154-158 (1987)

Fonseca LM, El-Halal SLM, Dias ARG, Zavareze EDR. Physical modification of starch by heat-moisture treatment and annealing and their applications: A review. Carbohydrate Polymers. 274: 118665 (2021)

Gou M, Wu H, Saleh ASM, Jing L, Liu Y, Zhao K, Su C, Zhang B, Jiang H, Li W. Effects of repeated and continuous dry heat treatments on properties of sweet potato starch. International Journal of Biological Macromolecules. 129: 869-877 (2019)

Han X, Kang J, Bai Y, Xue M, Shi YC. Structure of pyrodextrin in relation to its retrogradation properties. Food Chemistry. 242: 169-173 (2018)

Hong JS, Chung HJ, Lee BH, Kim HS. Impact of static and dynamic modes of semi-dry heat reaction on the characteristics of starch citrates. Carbohydrate Polymers. 233: 115853 (2020)

Kim HS, Huber KC. Physicochemical properties and amylopectin fine structures of A- and B-type granules of waxy and normal soft wheat starch. Journal of Cereal Science. 51: 256-264 (2010)

Kim RJ, Kim HS. Development and characterization of potato amylopectin-substituted starch materials. Food Science and Biotechnology. 30: 833-842 (2021)

Kim HS, Kim BY, Baik MY. Application of ultra high pressure (UHP) in starch chemistry. Critical Reviews in Food Science and Nutrition. 52: 123-141 (2012)

Lim ST, Han JA, Lim HS, BeMiller JN. Modification of starch by dry heating with ionic gums. Cereal Chemistry. 79: 601-606 (2002)

Lim HS, BeMiller JN, Lim ST. Effect of dry heating with ionic gums at controlled pH on starch pasting viscosity. Cereal Chemistry. 80: 198-202 (2003)

Liu K, Hao Y, Chen Y, Gao Q. Effects of dry heat treatment on the structure and physicochemical properties of waxy potato starch. International Journal of Biological Macromolecules. 132: 1044-1050 (2019)

Mao H, Chen Z, Li J, Zhai X, Li H, Wen Y, Wang J, Sun B. Structural comparisons of pyrodextrins during thermal degradation process: The role of hydrochloric acid. Food Chemistry. 349: 129174 (2021)

Mao H, Li J, Chen Z, Yan S, Li H, Wen Y, Wang J. Molecular structure of different prepared pyrodextrins and the inhibitory effects on starch retrogradation. Food Research International. 143: 110305 (2021)

Obadi M, Xu B. Review on the physicochemical properties, modifications, and applications of starches and its common modified forms used in noodles products. Food Hydrocolloids. 112: 106286 (2021)

Park S, Kim YR. Clean label starch: production, physicochemical characteristics, and industrial applications. Food Science and Biotechnology. 30: 1-17 (2021)

Qiu C, Cao J, Xiong L, Sun Q. Differences in physicochemical, morphological, and structural properties between rice starch and rice flour modified by dry heat treatment. Starch-Stäke. 67: 756-764 (2015)

Qin Y, Liu C, Jiang S, Cao J, Xiong L, Sun Q. Functional properties of glutinous rice flour by dry-heat treatment. PloS ONE. 11: e0160371 (2016)

Shi X, BeMiller JN. Effects of food gums on viscosities of starch suspensions during pasting. Carbohydrate Polymers. 50: 7-18 (2002)

Sitohy MZ, Labib SM, El-Saadany SS, Ramadan MF. Optimizing the conditions for starch dry phosphorylation with sodium mono- and dihydrogen orthophosphate under heat and vacuum. Starch-Stäke. 52: 95-100 (2000)

Sun Q, Gong M, Li Y, Xiong L. Effect of dry heat treatment on the physicochemical properties and structure of proso millet flour and starch. Carbohydrate Polymers. 110: 128-134 (2014)

Weil W, Weil RC, Keawsompong S, Sriroth K, Seib PA, Shi YC. Pyrodextrin from waxy and normal tapioca starches: Physicochemical properties. Food Hydrocolloids. 104: 105745 (2020)

Ye J, Hu X, Luo S, Liu W, Chen J, Zeng Z, Liu C. Properties of starch after extrusion: A review. Starch-Stäke. 70: 1700110 (2018)

Yousif EI, Gadallah MGE, Sorour AM. Physico-chemical and rheological properties of modified con starches and its effect on noodle quality. Annals of Agricultural Sciences. 57: 19-27 (2012)

Zhou YL, Cui LH, You XY, Jiang ZH, Qu WH, Liu PD, Ma DY, Cui YY. Effects of repeated and continuous dry heat treatments on the physicochemical and structural properties of quinoa starch. Food Hydrocolloids. 113: 106532 (2021)